

# Diffusion Filters for Separation of Solvent–Protein and Protein–Protein Nuclear Overhauser Effects (HYDRA)

Gerhard Wider, Roland Riek, and Kurt Wüthrich\*

Contribution from the Institut für Molekularbiologie und Biophysik, Eidgenössische Technische Hochschule-Hönggerberg, CH-8093 Zürich, Switzerland

Received March 5, 1996<sup>⊗</sup>

**Abstract:** Nuclear magnetic resonance (NMR) spectroscopy in solution has a unique potential for providing novel insights into structural and dynamic aspects of the solvation of biological macromolecules such as proteins, which is based on the observation of intermolecular solvent–protein nuclear Overhauser effects (NOEs) in the laboratory frame and the rotating frame. In these experiments spectral overlap between resonance lines of the solvent and the macromolecule may make the distinction between certain water–protein and protein–protein NOEs ambiguous even in two- and higher-dimensional NMR experiments. Here we show that use of diffusion filters in NOE difference experiments enables the observation of hydration water molecules without interference from intramolecular NOEs. Water–protein NOEs can thus be unambiguously identified from measurements at a single set of solution conditions. The proposed approach works well also with very short mixing times, and the resulting spectra are easy to analyze. One-dimensional experiments with diffusion filters have been combined with higher-dimensional experiments to obtain the chemical shift dispersion needed for individual resonance assignments.

## Introduction

During the past few years, NMR<sup>1</sup> methods based on NOE and ROE measurements have been developed to study interactions of individual protons in biological macromolecules with hydration water or other solvent molecules.<sup>2–4</sup> This NMR approach has the unique potential to combine atomic resolution determination of hydration sites in the three-dimensional macromolecular structures with information on dynamic aspects of biomolecular hydration.<sup>3,5,6</sup> In this paper we address a technical limitation which is ubiquitous in high-resolution NMR studies of the hydration of macromolecules such as proteins: the water line and some protein resonances usually overlap.<sup>7</sup> This makes the distinction between water–protein interactions, which may include NOEs as well as chemical exchange, and intraprotein <sup>1</sup>H–<sup>1</sup>H NOEs difficult. Even in 2D or 3D NMR experiments the unambiguous assignment of water–protein interactions is then often not possible in a single experiment. In uniformly <sup>15</sup>N, <sup>13</sup>C isotope-enriched proteins, intramolecular NOEs can be suppressed using <sup>15</sup>N- and <sup>13</sup>C-filtering techniques,<sup>8</sup> but

unless the level of enrichment reaches 100% there remains a risk of “breakthrough” of intramolecular NOEs.<sup>9</sup> It is therefore highly desirable that the first step in a NMR pulse sequence for hydration studies consist of a 1D NMR experiment that selects strictly for intermolecular protein–water interactions. For this purpose a variety of schemes were proposed which are based on selective excitation of the water resonance.<sup>10,11</sup> Selective excitation works well as long as there is no chemical shift overlap between the solvent and resonance lines from the macromolecule. Otherwise, distinction of solvent–protein NOEs from all intramolecular NOEs may not be possible because the excitation profiles of the available selective pulses, and even of radiation damping, are typically too wide. To resolve the ensuing ambiguities in resonance assignments, careful analysis of multiple measurements at different conditions, in particular at different temperatures, is often employed.

Here, we describe a novel 1D NMR difference experiment, HYDRA, in which the separation of intermolecular solvent–protein NOEs and chemical exchange effects from intramolecular NOEs is based on the different diffusion properties of individual water molecules and the biological macromolecules.<sup>12</sup> HYDRA contains strictly only water–protein interactions. For practical applications it can be used as a platform for relays by higher-dimensional experiments with improved peak separation.

In liquids, translational diffusion during a time interval  $\Delta$  results in different NMR signal intensities depending on whether or not  $\Delta$  is bounded by two identical pulsed magnetic field gradients (PFG), leading to signal intensities with (*S*) and

<sup>⊗</sup> Abstract published in *Advance ACS Abstracts*, October 15, 1996.

(1) Abbreviations: NMR, nuclear magnetic resonance; NOE, nuclear Overhauser effect; ROE, NOE in the rotating frame; 2D, 2-dimensional; PFG, pulsed field gradient; NOESY, 2D NOE spectroscopy; BPTI, basic pancreatic trypsin inhibitor; COSY, 2D correlation spectroscopy; TOCSY, 2D total correlation spectroscopy; ROESY, 2D ROE spectroscopy; HYDRA, NOE difference experiment using diffusion filters to distinguish between the resonances of hydration water and those of a macromolecular solute; HYDRA-N, HYDRA-R, HYDRA experiments in the laboratory frame and the rotating frame, respectively.

(2) Otting, G.; Wüthrich, K. *J. Am. Chem. Soc.* **1989**, *111*, 1871–1875.

(3) Otting, G.; Liepinsh, E.; Wüthrich, K. *Science* **1991**, *254*, 974–980.

(4) Dötsch, V.; Wider, G.; Siegal, G.; Wüthrich, K. *FEBS Lett.* **1995**, *366*, 6–10. Liepinsh, E.; Otting, G. *J. Am. Chem. Soc.* **1994**, *116*, 9670–9674. Wüthrich, K. In *Toward a Molecular Basis of Alcohol Use and Abuse*; Jansson, B., Jörnvall, H., Rydberg, U., Terenius, L., Vallee, B. L., Eds.: Birkhäuser: Basel, 1994; pp 261–268.

(5) Wüthrich, K. *Cold Spring Harbor Symp. Quant. Biol.* **1993**, *58*, 149–157.

(6) Dötsch, V.; Wider, G. *J. Am. Chem. Soc.* **1995**, *117*, 6064–6070.

(7) Wüthrich, K. *NMR of Proteins and Nucleic Acids*; Wiley: New York, 1986.

(8) Otting, G.; Wüthrich, K. *Q. Rev. Biophys.* **1990**, *23*, 39–96.

(9) Grzesiek, S.; Bax, A.; Nicholson, L. K.; Yamazaki, T.; Wingfield, P.; Stahl, S. J.; Eyermann, C. J.; Torchia, D. A.; Hodge, C. N.; Lam, P. Y. S.; Jadhav, P. K.; Chang, C. H. *J. Am. Chem. Soc.* **1994**, *116*, 1581–1582.

(10) Otting, G.; Liepinsh, E. *J. Biomol. NMR* **1995**, *5*, 420–426.

(11) Qi, P. X.; Urbauer, J. L.; Fuentes, E. J.; Leopold, M. F.; Wand, A. *J. Nature Struct. Biol.* **1994**, *1*, 378–381. Mori, S.; Johnson, M. O.; Berg, J. M.; Van Zijl, P. C. M. *J. Am. Chem. Soc.* **1994**, *116*, 11982–11984. Dalvit, C.; Hommel, U. *J. Biomol. NMR* **1995**, *5*, 306–310.

(12) Kriwacki, R. W.; Hill, R. H.; Flanagan, J. M.; Caradonna, J. P.; Prestegard, J. H. *J. Am. Chem. Soc.* **1993**, *115*, 8907–8911.

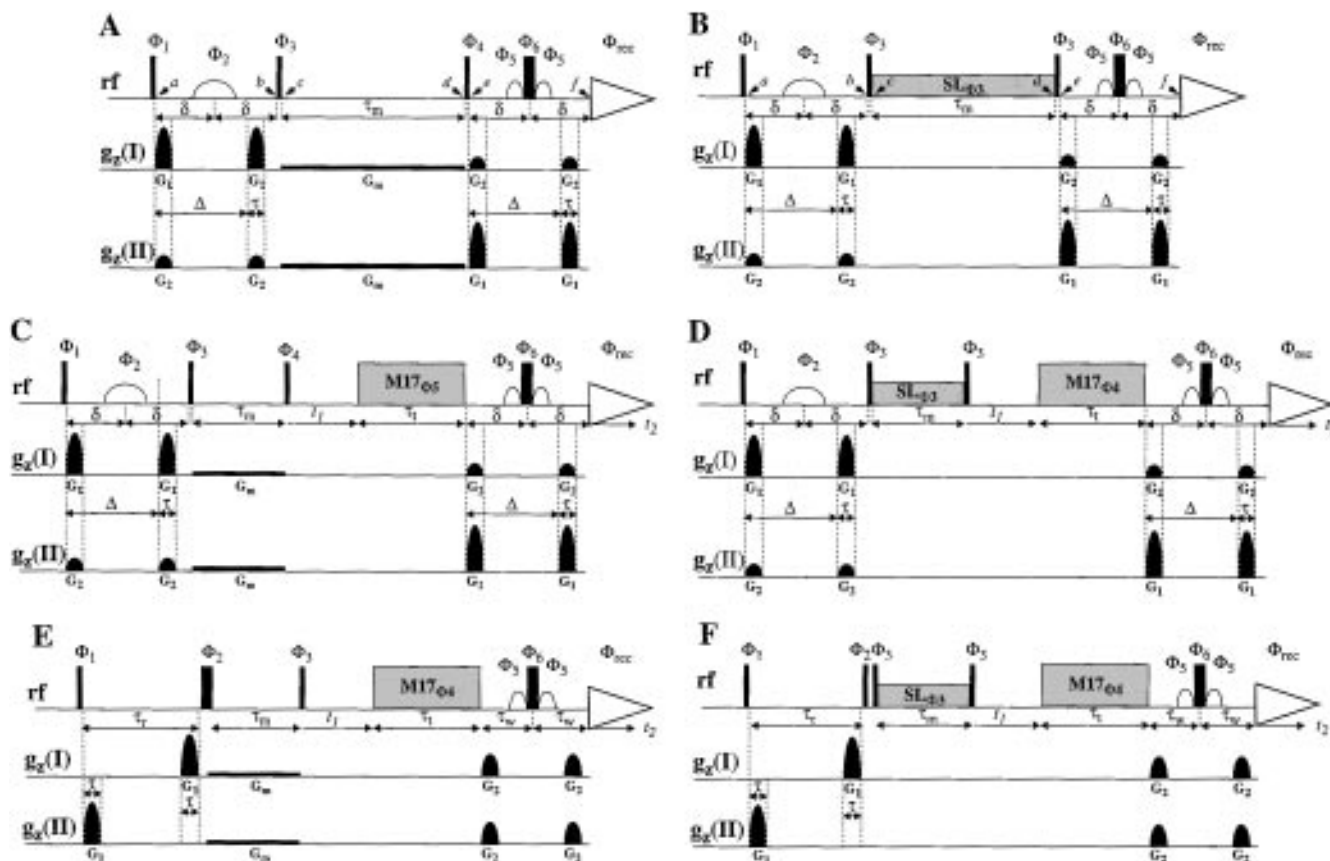


**Figure 1.** Experimental schemes for HYDRA-N and HYDRA-R NOE difference experiments with diffusion filters for separation of water–protein and protein–protein NOEs (A–D) and two corresponding experiments using radiation damping for selection of the water resonance (E, F). On the line rf (radio frequency), wide and narrow bars stand for hard 180° and 90° pulses, respectively, and the curved shapes indicate selective pulses at the water frequency. The phases of the individual rf pulses are given at the top. In A and B discrete time points are identified by a–f. For the HYDRA experiments (A–D) the selective 180° pulse with phase  $\Phi_2$  is centered between a and b in the period of length  $2\delta$ , and  $\tau_m$  indicates the NOE mixing time. The second diffusion filter immediately before the acquisition is combined with a WATERGATE sequence<sup>18</sup> to suppress the water resonance. The lines  $g_z(I)$  and  $g_z(II)$  indicate the applied magnetic field gradients; the desired spectrum corresponds to the difference between two subsequent experiments recorded with  $g_z(I)$  and  $g_z(II)$ , respectively. Each gradient has a modified rectangular shape to reduce the magnetic field instabilities, with the first quarter having a  $\sin^2$  shape and the last quarter a  $\cos^2$  dependence.<sup>6,14</sup> The individual gradient strengths are indicated by  $G_1$ ,  $G_2$ , and  $G_m$ , where  $G_1$  is strong,  $G_2$  is weak, and  $G_m$  is very weak. The length of the  $G_1$  and  $G_2$  gradients is  $\tau$ ;  $G_m$  is applied continuously during the NOE mixing time.  $\Delta$  is the diffusion time. The phase cycles are designed to result directly in the desired difference spectrum, using the two different gradient traces  $g_z(I)$  and  $g_z(II)$  in alternate scans. Quadrature detection in  $t_1$  is obtained by alternating the phases  $\Phi_4$  in C,  $\Phi_3$  in D and E, and  $\Phi_2$  and  $\Phi_3$  in F according to States-TPPI.<sup>21</sup> A: 1D [ $^1H_S, ^1H_M$ ]-NOE difference experiment ( $H_S$  is a solvent proton and  $H_M$  a hydrogen atom of the macromolecule) in the laboratory frame (HYDRA-N). Phase cycling:  $\Phi_1 = 4x, 4y$ ;  $\Phi_2 = 2(4x, 4y), 2(4(-x), 4(-y))$ ;  $\Phi_3 = 2(-x), 2x, 2(-y), 2y$ ;  $\Phi_4 = 4(-x), 4(-y), 4x, 4y$ ;  $\Phi_5 = \Phi_4$ ;  $\Phi_6 = 4x, 4y, 4(-x), 4(-y)$ ;  $\Phi_{rec} = y, 2(-y), y, -x, 2x, -x, -y, 2y, -y, x, 2(-x), x$ . B: 1D [ $^1H_S, ^1H_M$ ]-NOE difference experiment in the rotating frame (HYDRA-R); SL is a ROE spin–lock mixing sequence. Phase cycling:  $\Phi_1 = 8(2x, 2y), 8(2(-x), 2(-y))$ ;  $\Phi_2 = 4(2x, 2y), 4(2(-x), 2(-y))$ ;  $\Phi_3 = 2y, 2(-x), 2(-y), 2x$ ;  $\Phi_5 = 2(2(-x), 2(-y)), 2(2x, 2y)$ ;  $\Phi_6 = 2(2x, 2y), 2(2(-x), 2(-y))$ ;  $\Phi_{rec} = 8(y, -y, -x, x), 8(-y, y, x, -x)$ . C: 2D TOCSY-related HYDRA-N experiment; M17 is a MLEV-17 TOCSY mixing sequence of duration  $\tau_m$ , including a trim pulse of 2 ms length at the start and a trim pulse of 1.3 ms at the end of the mixing sequence. Phase cycling:  $\Phi_1 = 4x, 4y$ ;  $\Phi_2 = 2(4x, 4y), 2(4(-x), 4(-y))$ ;  $\Phi_3 = 2(-x), 2x, 2(-y), 2y$ ;  $\Phi_4 = 4(-x), 4(-y), 4x, 4y$ ;  $\Phi_5 = 4x, 4y, 4(-x), 4(-y), 4(-x), 4(-y), 4x, 4y$ ;  $\Phi_6 = 4(-x), 4(-y), 4x, 4y, 4x, 4y, 4(-x), 4(-y)$ ;  $\Phi_{rec} = y, 2(-y), y, -x, 2x, -x, -y, 2y, -y, x, 2(-x), x$ . D: 2D TOCSY-related HYDRA-R experiment. Phase cycling:  $\Phi_1 = 8(2x, 2y), 8(2(-x), 2(-y))$ ;  $\Phi_2 = 4(2x, 2y), 4(2(-x), 2(-y))$ ;  $\Phi_3 = 2y, 2(-x), 2(-y), 2x$ ;  $\Phi_4 = 4(2x, 2y), 4(2(-x), 2(-y))$ ;  $\Phi_5 = 2(2(-x), 2(-y)), 2(2x, 2y)$ ;  $\Phi_6 = 2(2x, 2y), 2(2(-x), 2(-y))$ ;  $\Phi_{rec} = 8(y, -y, -x, x), 8(-y, y, x, -x)$ . E: 2D TOCSY-related [ $^1H, ^1H$ ]-NOE experiment using radiation damping for selection of the water resonance;  $\tau_r$  is the time period during which radiation damping is effective, and  $\tau_w$  is the half-duration of the application of WATERGATE. Phase cycling:  $\Phi_1 = 4x, 4y$ ;  $\Phi_2 = 4(-x), 4(-y), 4x, 4y$ ;  $\Phi_3 = 2(-x), 2x, 2(-y), 2y$ ;  $\Phi_4 = 4x, 4y, 4(-x), 4(-y), 4(-x), 4(-y), 4x, 4y$ ;  $\Phi_5 = 4x, 4y, 4(-x), 4(-y), 4(-x), 4(-y), 4x, 4y$ ;  $\Phi_6 = 4(-x), 4(-y), 4x, 4y, 4x, 4y, 4(-x), 4(-y)$ ;  $\Phi_{rec} = y, 2(-y), y, -x, 2x, -x$ . F: 2D TOCSY-related [ $^1H, ^1H$ ]-ROE experiment using radiation damping for selection of the water resonance. Phase cycling:  $\Phi_1 = 2x, 2y$ ;  $\Phi_2 = 2x, 2y$ ;  $\Phi_3 = 2y, 2(-x), 2(-y), 2x$ ;  $\Phi_4 = 4(2x, 2y), 4(2(-x), 2(-y))$ ;  $\Phi_5 = 2(2(-x), 2(-y)), 2(2x, 2y)$ ;  $\Phi_6 = 2(2x, 2y), 2(2(-x), 2(-y))$ ;  $\Phi_{rec} = y, -y, -x, x$ .

without ( $S_0$ ) gradients according to<sup>13</sup>

$$\frac{S}{S_0} = \exp\left[-\gamma^2 \tau^2 G^2 \left(\Delta - \frac{\tau}{3}\right) D\right] \quad (1)$$

where  $D$  is the translational diffusion coefficient,  $\gamma$  is the gyromagnetic ratio ( $26.7519 \times 10^7 \text{ rad T}^{-1} \text{ s}^{-1}$  for protons),  $\tau$

is the length of the gradient,  $G$  is the gradient strength, and  $\Delta$  is the time period between the two gradients (Figure 1). As a rule, water molecules diffuse about 15–20 times faster than proteins in the molecular weight range 10–20 kDa. For example, the self-diffusion constants of  $H_2O$  and the protein BPTI in a 20 mM BPTI solution in 90%  $H_2O/10\%$   $D_2O$  at 4 °C are  $1.0 \times 10^{-5}$  and  $1.2 \times 10^{-6} \text{ cm}^2/\text{s}$ , respectively.<sup>14</sup> On this basis, intermolecular water–protein NOEs can be distin-

guished from intramolecular NOEs with the use of a diffusion filter<sup>15</sup> in the NOESY pulse sequence. A suitably designed experiment, which measures the difference between the signals obtained with strong and weak PFGs in a diffusion filter, selectively records intermolecular protein–water interactions. This approach can be used for a wide range of NOE mixing times, including the very short values that are typically required for studies of surface hydration in the presence of spin diffusion from interior hydration water molecules and from exchanging protons of amino acid side chains or nucleic acid riboses and bases.<sup>16,17</sup>

## Materials and Methods

The experimental schemes presented in Figure 1 were used with solutions of BPTI, which is a protein with molecular weight 6 kDa, in a mixture of 90% H<sub>2</sub>O/10% D<sub>2</sub>O at a temperature of 277 K. All experiments were performed on a Bruker AMX 500 NMR spectrometer equipped with a *z*-gradient probehead and a 30 A gradient amplifier which can deliver PFGs with a strength of up to 150 G/cm.

Figure 1A shows the pulse sequence for the new 1D HYDRA experiment in the laboratory frame (HYDRA-N). Overall, HYDRA-N consists of the NOE mixing period,  $\tau_m$ , sandwiched between two diffusion filters. The difference between the data measured in alternating scans using the gradient traces  $g_z(I)$  and  $g_z(II)$ , respectively, is the desired water–protein interaction spectrum. The delay  $\Delta$  and the gradient strengths  $G_1$  and  $G_2$  are chosen such that with  $G_1$  most of the water magnetization is destroyed by diffusion, whereas with  $G_2$  most of the water magnetization is preserved. The actual gradient strengths depend on the difference between the diffusion constants of the solvent and the solute, and eq 1 is used to optimize the choice of  $G_1$  and  $G_2$ . Most of the protein magnetization is destroyed by the gradients between the time points *a* and *b* because the selective 180° pulse refocuses only a narrow frequency band centered about the water resonance, so that only macromolecular resonances close to the water are preserved and the subtraction properties of the experiment are improved, which is especially important for the methyl signals. The intensities of the intramolecular NOEs of these remaining protein protons at point *e* in Figure 1A are different for the gradient traces  $g_z(I)$  and  $g_z(II)$ , but this difference is compensated by the inverted diffusion weighting in the second diffusion filter. Complete cancellation at time *f* in Figure 1A is thus assured when subtracting the two measurements (I and II) from each other. This is in contrast with the fate of the NOEs between water and protein protons. The water magnetization along the negative *z*-axis at the beginning of the mixing time (*c* in Figure 1A) is small in the presence of strong  $G_1$  gradients, and therefore the intensities of the NOEs to the protein protons are small. For weak gradients  $G_2$  the corresponding intensities will be much larger. Most of the NOE intensity between water and protein protons will therefore be retained in the difference spectrum. For the suppression of the residual water before acquisition, the second diffusion filter is combined with a WATERGATE sequence.<sup>18</sup> In devising the phase cycling given in the caption to Figure 1, which yields directly the difference spectrum when using the gradient traces  $g_z(I)$  and  $g_z(II)$  in alternate scans, consideration had to be given to the fact that the same amount of magnetization from protein protons that relax during the mixing time (at time point *d* in Figure 1A) is present for both gradient strengths  $G_1$  and  $G_2$  used for the first diffusion filter. Due to the different strengths of  $G_1$  and  $G_2$  in the second diffusion filter, this would result in a non-zero difference spectrum. For this reason the phase cycle  $\Phi_3$  was doubled to bring the water magnetization at the start of the mixing time (*c* in Figure 1A) into the +*z* direction in half of the scans, which allows subtraction of the residual difference caused by the relaxed protein magnetization.

(14) Wider, G.; Dötsch, V.; Wüthrich, K. *J. Magn. Reson.* **1994**, *A108*, 255–258.

(15) Van Zijl, P. C. M.; Moonen, C. *J. Magn. Reson.* **1990**, *87*, 18–25.

(16) Otting, G.; Liepinsh, E.; Farmer, B. T., II; Wüthrich, K. *J. Biomol. NMR* **1991**, *1*, 209–215.

(17) Liepinsh, E.; Otting, G.; Wüthrich, K. *J. Biomol. NMR* **1992**, *2*, 447–465.

(18) Piotto, M.; Saudek, V.; Sklenar, V. *J. Biomol. NMR* **1992**, *2*, 661–665.

Figure 1B shows the pulse sequence for the 1D HYDRA experiment in the rotating frame (HYDRA-R). This scheme differs from HYDRA-N by replacement of the NOE mixing time by a ROE spin–lock sequence during  $\tau_m$ , by removal of the gradient  $G_m$  and by different phase cycling (see legend to Figure 1). In HYDRA-R there is no relaxed protein magnetization at the end of  $\tau_m$  (*d* in Figure 1B), so that in contrast to HYDRA-N the phase cycle does not need to be doubled.

To achieve the spectral resolution needed for obtaining individual assignments of water–protein interactions, the basic 1D HYDRA schemes can be combined with higher-dimensional experiments, such as 2D [<sup>1</sup>H,<sup>1</sup>H]-COSY, -TOCSY, or -NOESY, or heteronuclear experiments with labeled proteins. Figure 1C,D shows combinations of HYDRA-N and HYDRA-R with [<sup>1</sup>H,<sup>1</sup>H]-TOCSY. In these experiments the magnetization transfer during the NOE or ROE mixing time is relayed to scalar coupled protons in the amino acid spin systems. To this end the evolution period and the TOCSY mixing sequence have been inserted in HYDRA between the NOE mixing time and the second diffusion filter, which is again combined with WATERGATE to suppress the water resonance.

Optimization of the gradients  $G_1\tau$  and  $G_2\tau$  in the diffusion filters used in HYDRA experiments is based on the fact that if  $G_1\tau$  is chosen small enough to bring the signal attenuation for both the water and the protein very close to zero (eq 1), then a maximal NOE signal is obtained for the largest difference between signal attenuation of the water and the protein by the diffusion filter with the power gradient  $G_2\tau$  (Figure 1A). Using eq 1 and assuming that  $\tau/3 \ll \Delta$ , so that  $\Delta - \tau/3$  can be replaced by  $\Delta$ , expression 2 for the gradient power  $G_2\tau$  can be derived,

$$G_2\tau = \sqrt{(-\ln k)/((1-k)\gamma^2\Delta D_w)} \quad (2)$$

where  $D_w$  is the translational diffusion coefficient of water and  $k$  is the ratio between the translational diffusion coefficient of the protein and  $D_w$ . For example,  $G_2\tau = 0.2$  Gs/cm for  $k = 1/15$ ,  $D_w = 10^{-5}$  cm<sup>2</sup>/s, and  $\Delta = 10$  ms. With  $G_2 = 100$  G/cm, one obtains  $\tau = 2$  ms, and with the same value of  $\tau$ , the gradient  $G_1$  can be chosen up to 8 G/cm to satisfy the initial condition of eq 2. This optimization does not consider spin relaxation during the diffusion filters, which may be of concern during the second diffusion filter, depending on the values of the delay  $\Delta$  and the proton relaxation rate. For proteins, the total duration of the diffusion filters should be short to minimize relaxation losses, which calls for the use of the high gradient strengths.

Compared to techniques based on selective excitation,<sup>10,11,20</sup> the introduction of diffusion filters reduces the sensitivity. There are signal losses due to diffusion, depending on the ratio of the translational diffusion coefficients for the water and the protein. In the above example a diffusion filter with the gradient power of  $G_2\tau = 0.2$  Gs/cm will retain 82% of the protein magnetization and 6% of the water magnetization. In this typical case, HYDRA has about 75% of the sensitivity of a corresponding experiment using radiation damping. Both HYDRA and radiation-damping techniques are difference methods which are inherently less sensitive by a factor of 1.4 than methods using selective pulses on the water resonance.<sup>20</sup> Despite the reduced sensitivity, HYDRA will probably be the method of choice whenever the suppression of intramolecular NOEs is important, since for HYDRA suppression of intramolecular NOEs is independent of parameters such as temperature, pH, and relaxation times. In cases where interference by intramolecular NOEs is not of prime concern, techniques with higher sensitivity<sup>10,11,20</sup> (e.g., Figure 1E,F) may be preferable. The sensitivity of experiments used for the study of water–protein interactions, including HYDRA, could be improved using water flip-back methods.<sup>19</sup> However, for homonuclear spectroscopy these methods do not find widespread applications due to interference with the overall performance of the experiments, and the addition of a relaxation agent may therefore be a good compromise for measuring water–protein interactions.<sup>10</sup> For heteronuclear experiments, on the other hand, flip-back methods should be implemented.

To record a meaningful reference for assessing the new [<sup>1</sup>H,<sup>1</sup>H]-TOCSY-relayed HYDRA-N experiment, we devised the [<sup>1</sup>H,<sup>1</sup>H]-TOCSY-relayed NOE difference experiment of Figure 1E, which

(19) Grzesiek, S.; Bax, A. *J. Am. Chem. Soc.* **1993**, *115*, 12593–12594.

(20) Dalvit, C.; Hommel, U. *J. Magn. Reson. B* **1995**, *109*, 334–338.

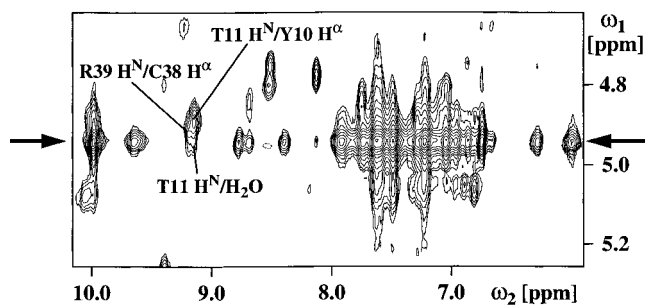


**Figure 2.** Region ( $\omega_1 = 4.6\text{--}5.2$  ppm,  $\omega_2 = 6.0\text{--}10.0$  ppm) of a 2D  $^1\text{H}$ ,  $^1\text{H}$ -NOESY spectrum recorded with a mixing time of 60 ms in a 10 mM BPTI solution in 90%  $\text{H}_2\text{O}/10\%$   $\text{D}_2\text{O}$  at pH = 4.6 and  $T = 277$  K. The water resonance was suppressed before acquisition using WATERGATE.<sup>18</sup> The spectrum with a sweep width of 7042 Hz in both dimensions contains  $2048 \times 1024$  real data points obtained from transforming  $2048 \times 512$  complex time domain data points. In both dimensions a cosine window was applied prior to Fourier transformation, and the base line was corrected using trigonometric functions. All the spectra in Figures 2–5 were processed with the program PROSA.<sup>22</sup> The arrows indicate the water resonance position in the indirect dimension,  $\omega_1$ , where one observes numerous exchange peaks and water–protein NOEs.<sup>2</sup> The labeled NOESY cross peaks Thr 11  $\text{H}^{\text{N}}$ –Tyr 10  $\text{H}^{\alpha}$  and Arg 39  $\text{H}^{\text{N}}$ –Cys 38  $\text{H}^{\alpha}$ , which are overlapped with the Thr 11  $\text{H}^{\text{N}}$ – $\text{H}_2\text{O}$  NOE peak, have  $\text{H}^{\alpha}$  resonance positions very close to the water resonance, so that they are excited by the commonly used selective water excitation schemes (see Figure 3).

minimizes the contributions to the NOEs during the selection of the water resonance with radiation damping and allows the use of short effective NOE mixing times. In the first scan, using the gradient scheme  $g_z(\text{I})$ , radiation damping is used to turn the water magnetization back to the  $+z$ -axis after the initial  $90^\circ$  pulse, and all transverse magnetization is destroyed before the  $180^\circ$  pulse  $\Phi_2$ , which turns the water magnetization to the  $-z$ -axis at the start of the NOE mixing time. After the evolution time, a MLEV-17 sequence is used for the TOCSY transfer, and before acquisition the water magnetization is destroyed with WATERGATE. In the second scan, using the gradient scheme  $g_z(\text{II})$ , a PFG after the first  $90^\circ$  pulse destroys all transverse magnetization. The spectrum obtained as the difference between the two scans contains water–protein NOEs or exchange peaks and intramolecular NOEs correlating protein resonances within a very narrow frequency band centered about the water resonance. Most unwanted magnetization is destroyed before the NOE mixing time, which makes the scheme robust relative to difference artifacts. Figure 1F shows the scheme for a corresponding 2D  $^1\text{H}$ ,  $^1\text{H}$ -TOCSY-related ROE experiment with water selection by radiation damping.

## Results and Discussion

In this section we demonstrate with measurements with the 6 kDa protein BPTI that compared to other available experiments, the HYDRA experimental schemes of Figure 1A–D yield superior results in two of the technically most difficult situations encountered in NMR studies of the hydration of biological macromolecules. These are the unambiguous identification of intermolecular water–protein NOEs or chemical exchange interactions in the presence of protein resonances at or very near the water chemical shift and the detection of the very weak NOEs between short-lived surface hydration water and protein protons.<sup>3</sup>

The 2D  $^1\text{H}$ ,  $^1\text{H}$ -NOESY spectrum in Figure 2 introduces the system used to evaluate the potentialities of HYDRA for resolving overlapped resonances and provides a reference for assessing the performance of the new experiment (see Figure 3). The NOE cross peaks Arg 39  $\text{H}^{\text{N}}$ –Cys 38  $\text{H}^{\alpha}$  and Thr 11  $\text{H}^{\text{N}}$ –Tyr 10  $\text{H}^{\alpha}$  overlap with the NOE cross peak Thr 11  $\text{H}^{\text{N}}$ –water. In Figure 3 the cross section at the  $\omega_1$  position of the water resonance (arrows in Figure 2) through the NOESY

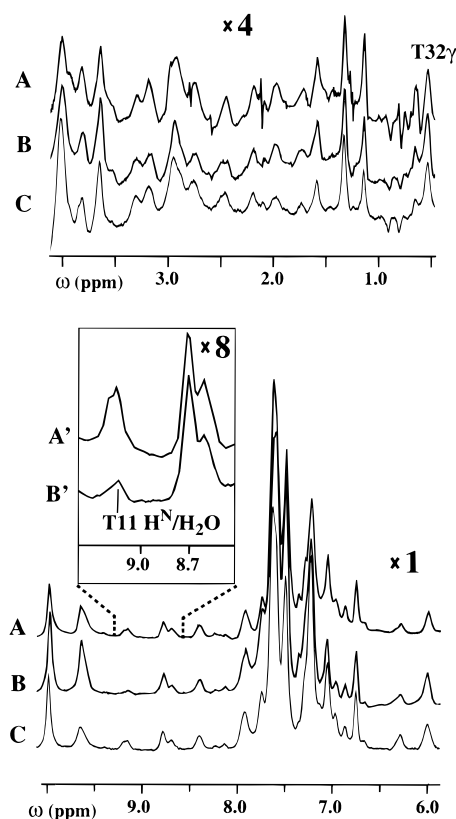


**Figure 3.** Regions from 0.5 to 4.0 and 6.0 to 10.0 ppm of NOE spectra recorded with different experimental schemes, showing interactions of water with protein protons. The data were recorded with a 10 mM solution of BPTI in 90%  $\text{H}_2\text{O}/10\%$   $\text{D}_2\text{O}$  at pH = 4.6 and  $T = 277$  K. Prior to Fourier transformation, 4096 time domain data points were zero-filled to 8192 points and multiplied by an exponential window using a line broadening factor of 5. The spectral region 0.5–4.1 ppm was scaled up by a factor of 4 compared to the region 6.0–10.1 ppm, which contains intense exchange peaks.<sup>2</sup> The intensities in the three spectra were calibrated relative to the cross peak between the water and the  $\gamma$ -methyl resonance of Thr 32. For all three measurements a relaxation delay of 1 s was used between scans, and the total measuring time was 3 h. A: Radiation damping was used for the selection of the water resonance.<sup>10</sup> All gradients used were rectangular, with a length of 1 ms and a strength of 15 G/cm, except that the gradients in WATERGATE were sine shaped with a maximum strength of 22.5 G/cm. The mixing time was 140 ms (including 80 ms for radiation damping). B: HYDRA-N experiment of Figure 1A, with  $\delta = 5.15$  ms. The lengths of the selective  $\pi$  and  $\pi/2$  rectangular pulses on the water were 4.1 and 1.9 ms, respectively; the NOE mixing time  $\tau_m = 60$  ms,  $G_1 = 115$  G/cm, and  $G_2 = 10$  G/cm, with gradient recovery times of 1 ms,  $\tau = 1.5$  ms,  $\Delta = 7.8$  ms,  $G_m = 2$  G/cm. C: 2D NOESY spectrum of Figure 2,  $\tau_m = 60$  ms. A cross section along  $\omega_2$  through the  $\omega_1$  frequency of the water resonance (arrows in Figure 2) is shown. The insert contains the region 8.5–9.4 ppm of the spectra A (A') and B (B') with an 8-fold expanded vertical scale.

spectrum of Figure 2 is compared with the 1D HYDRA-N spectrum obtained with the pulse sequence of Figure 1A and with the result of a 1D NOE experiment using radiation damping for the water selection.<sup>10</sup> Overall, the three spectra are very similar, except that differences in corresponding peak heights in the three experiments arise for protons that exchange with the water. Rapidly exchanging protons show reduced signal heights in the NOESY cross section at the  $\omega_1$  chemical shift of water, since line broadening in  $\omega_1$  reduces the apparent signal intensities. This effect is especially pronounced for the tyrosyl hydroxyl resonance at 9.6 ppm but can also be seen for the tyrosyl hydroxyl line near 10.0 ppm and the threonyl hydroxyl resonance near 6.0 ppm. Smaller differences in the intensities

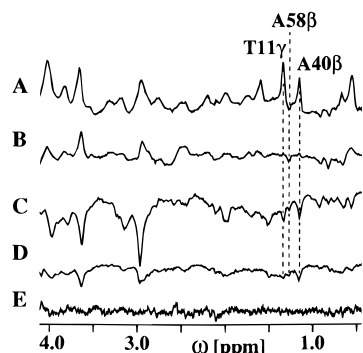


**Figure 4.** 1D HYDRA-N and HYDRA-R experiments recorded using the pulse schemes of Figure 1A,B with different mixing times. The same sample was used as in Figures 2 and 3, and the experimental parameters were the same as in Figure 3B. The resonance positions of the methyl groups of Ala 40, Ala 58, and Thr 11 are marked by dotted lines: (A) HYDRA-N with mixing time  $\tau_m = 60$  ms, 4096 scans accumulated; (B) HYDRA-N,  $\tau_m = 10$  ms, 8192 scans; (C) HYDRA-R,  $\tau_m = 30$  ms, 2048 scans; (D) HYDRA-R,  $\tau_m = 6$  ms, 4096 scans; (E) HYDRA-N, same conditions as in B but with presaturation of the water resonance during the 1 s relaxation delay to suppress all water–protein NOEs and exchange peaks. For this trace an 8-fold expanded vertical scale was used.

of exchange peaks are also visible between HYDRA and the experiment that uses radiation damping for solvent suppression. These arose because the effective mixing time in the latter experiment cannot readily be determined, and it was therefore important to normalize on the NOE peaks in the different spectra, which led to slight differences between the exchange peaks in Figure 3A,B. The spectral region containing the three overlapping cross peaks identified in Figure 2 is expanded in the insert. The differences between the traces A' and B' and A–C clearly demonstrate that the Thr 11  $H^N$ –water NOE, which is the only peak present in the HYDRA-N spectrum (Figure 3B,B'), is masked by the intramolecular protein–protein NOEs in the other two spectra, so that a correct evaluation of water–protein interactions in this spectral region is possible only in the HYDRA-N spectrum.

An additional advantage of HYDRA is that it can be used with very short ROE or NOE mixing times. This is in contrast to some schemes using radiation damping,<sup>10</sup> where mixing times of less than 60 ms cause severe loss in sensitivity and/or selectivity of the water excitation. Use of very short mixing times has previously been found to be necessary for studies of short-lived surface hydration, since the very weak NOEs between protein protons and surface hydration water would otherwise be masked by overlap with, or spin diffusion from, much stronger NOEs with interior water molecules or labile protein protons.<sup>3,16</sup> Figure 4A,B shows two HYDRA-N spectra obtained using the pulse sequence in Figure 1A with mixing times of 60 and 10 ms, respectively. We focus in the spectral analysis on the aliphatic region between 0.5 and 2.5 ppm. Many of the positive resonances in spectrum A are absent in Figure 4B, which is indicative of important contributions from spin diffusion in trace A. The strong resonances in Figure 4A have their origin in NOEs between nonlabile protein protons and either hydroxyl protons of Thr or the interior water molecules in BPTI.<sup>2,17</sup> The NOEs with the two methyl resonances of Ala 40 and Thr 11 are almost completely absent in the spectrum B, which enables unambiguous identification of the resonance line at the methyl position of Ala 58. This and several other peaks with a negative sign in Figure 4B are direct NOEs to surface hydration water molecules<sup>3</sup> which are hidden by the intense positive lines at longer mixing times. Figure 4E shows that these negative lines are not subtraction artifacts, since the same

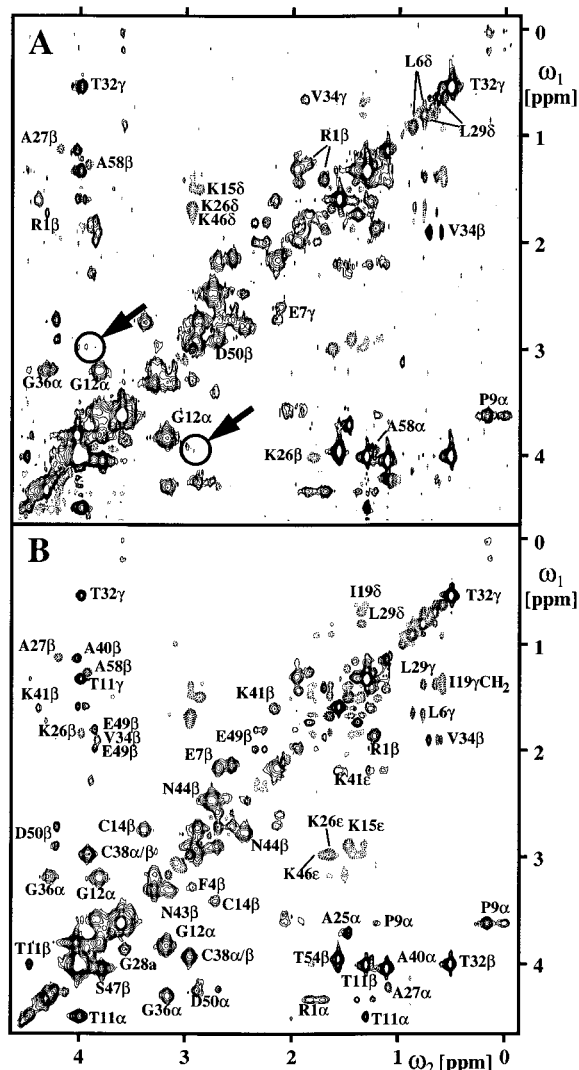


**Figure 5.** Contour plots of the spectral region ( $\omega_1 = 0$ –4.5 ppm,  $\omega_2 = 0$ –4.5 ppm) of 2D TOCSY-related NOE difference experiments. The NOE mixing time was  $\tau_m = 60$  ms, and the TOCSY mixing time was  $\tau_1 = 27$  ms. The sample used was 20 mM BPTI in 90%  $H_2O$ /10%  $D_2O$  at pH = 3.5 and  $T = 277$  K. Positive cross peaks are drawn with solid lines and negative cross peaks with dotted lines. A:  $[^1H, ^1H]$ -TOCSY-related HYDRA-N spectrum recorded with the pulse sequence of Figure 1C, using the same parameters as in Figure 3B;  $t_{1max} = 23.2$  ms, 768 scans per  $t_1$  increment; circles and arrows indicate the positions where the TOCSY-related NOE cross peaks Cys 38  $H^\alpha$ –Cys 38  $H^\beta$  would be observed. B:  $[^1H, ^1H]$ -TOCSY-related NOE difference spectrum recorded using radiation damping for selection of the water resonance (Figure 1E), recorded with  $t_{1max} = 30.7$  ms,  $\tau_r = 40$  ms,  $\tau_w = 3$  ms,  $\tau = 1$  ms,  $G_1 = 75$  G/cm,  $G_2 = 30$  G/cm, 320 scans accumulated per  $t_1$  increment, and otherwise the same parameters as in A. Cross peaks are identified with the protein proton interacting with the water or with the two protein protons interacting during the NOE mixing time, using the one-letter amino acid code, the sequence position, and greek letters to indicate the proton position. The assignments are adopted from ref 16. Some negative peaks in A are weaker than the corresponding peaks in B; this arises from the lower signal-to-noise ratio in A (see above) and the lower  $\omega_1$  resolution in A, which leads to some cancellation of signal intensity.

experiment as Figure 4B with water presaturation during the relaxation delay, which destroys all water–protein NOEs, contains no signals between 0.5 and 2.0 ppm. Figure 4C,D further shows two HYDRA-R spectra recorded with the scheme of Figure 1B. To account for the more rapid cross relaxation during the ROE mixing period, the mixing time was chosen one-half as long as in the HYDRA-N experiments, *i.e.*,  $\tau_m =$

30 ms (Figure 4C) and 6 ms (Figure 4D). Again, a much less intense resonance is observed for the methyl of Thr 11 at the shorter mixing time. The effect is less pronounced for Ala 40 because it overlaps with the methyl resonance of Ala 27. These resonances have opposite sign in HYDRA-N (see Figure 5), which leads to cancellation, but they have the same sign in HYDRA-R, which results in addition of their intensities.

Figure 5 compares a 2D [ $^1\text{H}$ ,  $^1\text{H}$ ]-TOCSY-relayed HYDRA-N spectrum recorded with the experiment of Figure 1C with a 2D [ $^1\text{H}$ ,  $^1\text{H}$ ]-TOCSY-relayed NOE experiment which uses radiation damping for the water selection (Figure 1E). This comparison documents that HYDRA-based higher-dimensional experiments can be applied simultaneously for unambiguous separation of water-protein interactions and intramolecular protein-protein NOEs and for detection of very weak NOEs with surface hydration water. In Figure 5A the diagonal comprises peaks which originate from water-protein NOEs or water-protein chemical exchange. The TOCSY relay transfers magnetization from the diagonal peaks to scalar coupled protons. Protons coupled to the proton manifesting a NOE peak on the diagonal then show a cross peak at the same  $\omega_1$  frequency as the diagonal peak. For example, the  $\alpha$ -proton of Pro 9 at  $\omega_1 = 3.7$  ppm,  $\omega_2 = 3.7$  ppm manifests an interaction with a water molecule, and the TOCSY relay peak to the  $\beta$ -protons of Pro 9 at  $\omega_1 = 3.7$  ppm,  $\omega_2 = 0.1$  ppm is therefore labeled P9 $\alpha$ . There is only a very weak symmetry-related peak at  $\omega_1 = 0.1$  ppm,  $\omega_2 = 3.7$  ppm so that the spectrum is asymmetric. If two coupled protons have a NOE to the same proton, or if there is spin diffusion, a symmetry-related peak appears, but it has in general different

intensity. Positive peaks correspond to signals that were previously assigned either to NOEs with the four interior water molecules in BPTI or to exchange peaks or NOEs with rapidly exchanging side chain hydroxyl protons of the protein.<sup>17</sup> Weak negative cross peaks manifest NOEs between water protons and solvent-accessible protons on the protein surface. The negative sign of the cross peaks shows that the vector connecting the interacting protons of the protein and the water undergoes spatial rearrangements in the fast motional regime, *i.e.*, with an effective correlation time  $< 0.5$  ns.<sup>3</sup> The spectrum of Figure 5A contains exclusively interactions with water protons, as is demonstrated by the absence of the TOCSY-relayed NOE between Cys 38  $\beta\text{CH}_2$  and Cys 38  $\text{H}^\alpha$ , which appears at the chemical shift positions of Cys 38  $\text{H}^{\beta 2}$  and Cys 38  $\text{H}^{\beta 3}$  (arrows in Figure 5A; see also Figure 2) in the spectrum of Figure 5B. This shows again that the HYDRA scheme implemented in the 2D [ $^1\text{H}$ ,  $^1\text{H}$ ]-TOCSY-relayed HYDRA-N experiment provides a clean separation of hydration interactions from intramolecular protein-protein NOEs, which is in contrast to the performance of other schemes presently available for this purpose.

**Acknowledgment.** We thank Mr. R. Marani for the careful processing of the manuscript and the Schweizerischer Nationalfonds for financial support (Project 31.32033.91).

JA9607188

(21) Marion, D.; Ikura, K.; Tschudin, R.; Bax, A. *J. Magn. Reson.* **1989**, *85*, 393–399.

(22) Güntert, P.; Dötsch, V.; Wider, G.; Wüthrich, K. *J. Biomol. NMR* **1992**, *2*, 619–629.